Analytical Methods

Accepted Manuscript

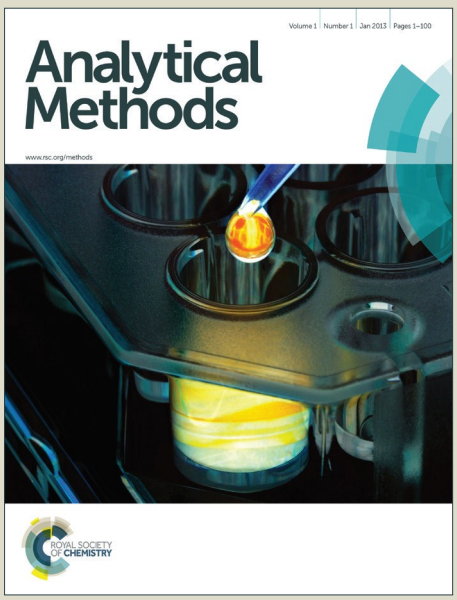

This is an *Accepted Manuscript*, which has been through the Royal Society of Chemistry peer review process and has been accepted for publication.

Accepted Manuscripts are published online shortly after acceptance, before technical editing, formatting and proof reading. Using this free service, authors can make their results available to the community, in citable form, before we publish the edited article. We will replace this *Accepted Manuscript* with the edited and formatted *Advance Article* as soon as it is available.

You can find more information about *Accepted Manuscripts* in the Information for Authors.

Please note that technical editing may introduce minor changes to the text and/or graphics, which may alter content. The journal's standard Terms & Conditions and the Ethical guidelines still apply. In no event shall the Royal Society of Chemistry be held responsible for any errors or omissions in this *Accepted Manuscript* or any consequences arising from the use of any information it contains.

ROYAL SOCIETY OF CHEMISTRY

www.rsc.org/methods

Photoelectrochemical aptasensor for mucin 1 based on DNA/aptamer linking of quantum dots and TiO_2 nanotube arrays

Jiuying Tian, Tao Huang and Jusheng Lu*

Jiangsu Key Laboratory of Green Synthetic Chemistry for Functional Materials, School of Chemistry and Chemical Engineering, Jiangsu Normal University, Xuzhou 221116, People's Republic of China

*Corresponding author at: School of Chemistry and Chemical Engineering, Jiangsu Normal University, 101 Shanghai Road, Xuzhou 221116, People's Republic of China Tel.: +86-516-83403165.

E-mail addresses: lujusheng@sina.com (J. S. Lu)

Abstract: Herein, a novel strategy for construction of a photoelectrochemical aptasensor for tumor marker mucin 1 (MUC1) was presented, which was based on the effective photoelectron transfer from CdTe quantum dots (QDs) to TiO_2 nanotube arrays (TiO_2 NTs) through DNA chain. First, we prepared a series of a TiO_2 NTs on titanium foil by the electrochemical anodization technique, and electrodeposited Au nanoparticles to improve the electrical conductivity and biocompatibility, which could load high amount of MUC1 aptamers by Au-S bond. Then, the synthetized c-DNA@QDs was immobilized on the TiO_2 NTs by hybridization of c-DNA and aptamer to form TiO_2 NT/aptamer/c-DNA@QD aptasensor. Detailed studies indicated that, under the irradiation of visible light, the aptasensor had good phocurrent response due to the excellent photosensitivity of CdTe QDs and electrical conductivity of DNA chain and Au/TiO_2 NTs. More importantly, the photocurrent response of the aptasensor was significantly affected by the TiO_2 NTs morphology and DNA chain length, which could be regulated by changing the tube length of TiO_2 NTs and the chain length of DNA linking QDs and TiO_2 NTs. Furthermore, the TiO_2 NT/aptamer/c-DNA@QD aptasensor for MUC1 exhibited good reproducibility and stability, wide linear range of 0.002-0.2 μM, and high sensitivity with LOD of 0.52 nM, which could be applied to the determination of MUC1 in human serum samples with good accuracy and recoveries. Therefore, the developed aptasensor could offer a promising feature for the analytical application in complex biological samples.

Introduction

Mucins encompass a family of high molecular weight, heavily O-glycosylated proteins that are differentially expressed in several epithelial malignancies. [1-3] The mucin 1 protein (MUC1) contains a hydrophobic membrane-spanning domain of 31 amino acids, acytoplasmic domain of 69 amino acids, and an extracellular domain consisting of a region of identical repeats of 20 amino acids per repeat, [4] which has been implicated in a variety of cancers, including breast, stomach, lung, prostate, colorectal and others. [5-7] Although a low level of expression of MUC1 could be found in healthy human serum (generally < 31 U mL^{-1} for healthy individuals which corresponds to approximately 5 μM for MUC1 [8, 9]), there is an up to 100-fold increase in the amount of mucin present on cancer cells compared to normal cells and MUC1 has a ubiquitous rather than focal cellular distribution. [10] Therefore, it is essential to derive analytical tools for monitoring MUC1 in patient samples for identifying the presence of submillimeter tumor masses. To date, there have many studies for MUC1 detection, in which, the aptamer-based assays are the main detection methods for MUC1. [9, 11-15] Aptamers which are artificial oligonucleotides in vitro selected through SELEX (systematic evolution of ligands by exponential enrichment), [16, 17] possess high affinity and high recognition ability for a wide array of targets. [18, 19] They are promising recognition elements for the development of ultrasensitive biosensors, for which the signal readout methods range from fluorescence spectroscopy to electrochemistry. For example, Yu et al. reported a MUC1 detection method was based on the fluorescence intensity of oligonucleotide-labeled quantum dots by MUC1 peptide. [10] Pang et al. performed an assay utilizing graphene oxide (GO) as a quencher able to quench the fluorescence of single-stranded dye-labeled MUC1 specific aptamer. [5] Liu et al. proposed a strategy for the sensitive detection of MUC1 based on

electrochemiluminescence resonance energy transfer (ERET) from Bis(2,2-bipyridine)-(5-aminophenanthroline) ruthenium (II) to GO. [11] Wu et al. reported the application of surface-enhanced Raman scattering spectroscopy for "trapping" human breast cancer cells using anti-MUC1 aptamer-Au/Ag nanoconjugates. [12] However, to our knowledge, there have little studies for the detection of MUC1 based on the combination of aptamer and photoelectrochemical (PEC) technique.

In PEC detection, light is utilized to excite the photoactive species and current is employed as the detection signal. Owing to the separation of excitation signal and detection signal, the PEC strategy has plenty of advantages such as low background, low potential different from electrochemiluminescence, which lead to a good analytical performance. [20-25] Among the photoactive materials, the semiconductor TiO_2 nanotube array grown on titanium foil is the most popular carriers used in PEC biosensing due to its photochemical stability, good biocompatibility and chemical stability, [26-29] and in particular, biocompatibility and negligible protein denaturation. [30, 31] However, TiO_2 has a wide band gap (3.2 eV) and can only be excited by ultraviolet light less than 380 nm, [32-34] which can kill biomolecules and limit its direct applications in PEC biosensing. In recent years, attempts have been made, including impurity doping, [35] metallization, [36] dye sensitization [37] or semiconductor quantum dots deposition, such as CdS, CdSe, PbS and CdTe, [38-41] to photosensitize TiO_2 for visible light response.

Herein, inspired by the unique PEC properties of TiO_2 nanotube arrays (TiO_2 NTs) and quantum dots (QDs), we developed a novel sensitive aptasensor for the tumor marker MUC1 based on PEC method. In details, as shown in Fig. 1, the TiO_2 NTs on titanium foil substrate were fabricated by the electrochemical anodization technique. The gold nanoparticles (AuNPs) were electrodeposited

in the tubes of TiO_2 NTs, which were favorable for improving the electrical conductivity of TiO_2 NTs and the MUC1 aptamers could be immobilized on the TiO_2 NTs by the Au-S bond. Then the CdTe QDs-labeled complementary single-stranded DNAs (c-DNA@QDs) were hybridized with the MUC1 aptamer to form a TiO_2 NT/aptamer/c-DNA@QD aptasensor. In the absence of target MUC1, under the irradiation of visible light, there have a high photocurrent response of the proposed aptasnesor due to the rich light absorption of CdTe QDs and the photoinduced electron transfer from CdTe QDs to TiO_2 NTs through DNA chain. However, in the presence of MUC1, MUC1 combined with its aptamer and CdTe QDs-labeled c-DNAs left the TiO_2 NTs, leading to the reduce of photocurrent. Therefore, the detection of target MUC1 could be sensitively transduced via detection of the photocurrent reduction.

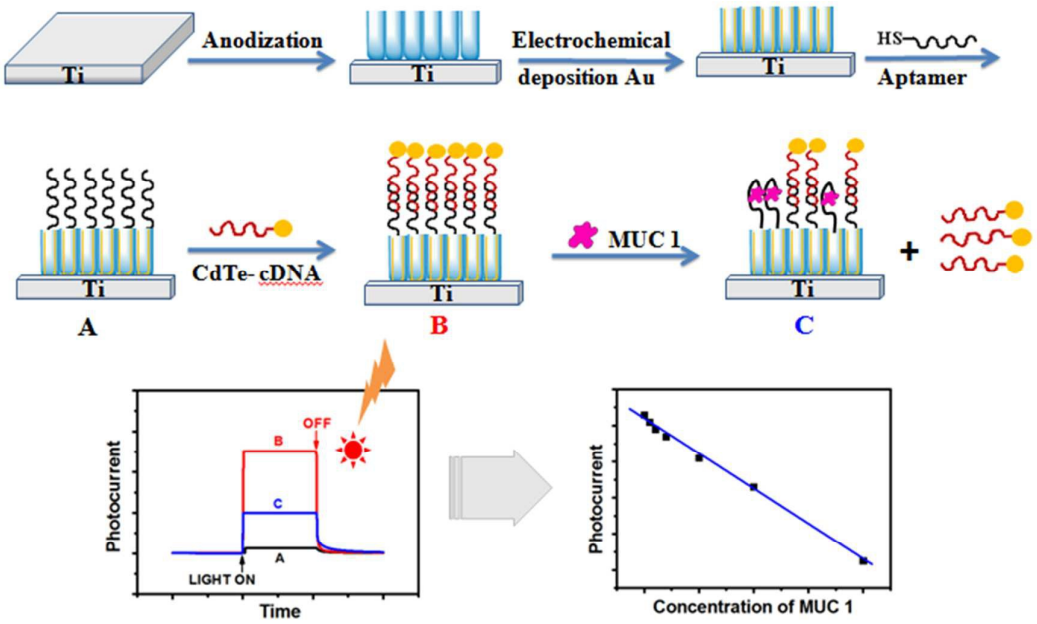

Fig. 1 Schematic representation of the TiO_2 NT/aptamer/c-DNA@QD photoelectrochemical aptasensor for the detection of MUC1.

Experimental

Materials and reagents

Titanium foils (99.7% purity) with a thickness of 0.127 mm, chloroauric acid ($HAuCl_4$), tellurium (powder, 200 mesh, 99.99%), sodium borohydride ($NaBH_4$, 99%), cadmium chloride hemi(pentahydrate) ($CdCl_2$, 99%), thiourea (97%), 3-mercaptopropionic acid (MPA, 99%), 1-ethyl-3-(3-dimethylaminopropyl) carbodiimide hydrochloride (EDC) and N-hydroxysuccinimide (NHS), were purchased from Sigma-Aldrich Co., Ltd. (St. Louis, MO, USA). Glycerol and NH_4F were obtained from Sinopharm Chemical Reagent Co., Ltd. (Shanghai, China).

MUC1 aptamer and corresponding c-DNA were synthesized by Sangon Biological Engineering Technology Co., Ltd. (Shanghai, China) and purified using high performance liquid chromatography. Their sequences were as following.

Thiolated MUC1 aptamer: 5'-HS-GCA GTT GAT C**CT TTG GAT A**CC CTG G-3'; c-DNA with complementary sequence (bold part) to aptamer: 5'-NH_2-$(TTT)_n$ TT**T ATC CAA AG**A-3'. Thiolated MUC1 aptamer and c-DNA were diluted to 10 μM in 10 mM phosphate buffer solution (PBS, pH 7.4) for use. The obtained solution was stored at 4 ^oC before use.

MUC1 (from the N terminus to the C terminus: APDTRPAPG) was purchased from Shanghai Apeptide Co., Ltd. The peptides were suspended in 10 mM pH 7.4 PBS to obtain different concentrations for the subsequent experiment. The preparation of AuNPs coated TiO_2 nanotube arrays was according to our previously reported method. [29] All other chemicals were of analytical grade and used as received. Deionized water (18.2 MΩ cm), obtained from a Milli-Q water purification system, was used in all experiments.

Apparatus

The anodization of titanium foils was carried out with DC power supply (WYK-1002, EKSI

Electric Manufacturing Co. Ltd, Jiangsu, China). The scanning electron micrographs were recorded with a field emission scanning electron microscopy (FESEM, Hitachi S-4800, Japan). The TEM images were performed by using transmission electron microscopy (JEOL Model JEM 2100, Japan). UV-vis absorption spectra were measured on a UV-2450 spectrometer (Shimadzu, Japan). Fluorescence spectra were measured on an F-4600 FL spectrophotometer (Hitachi, Japan).

Synthesis of CdTe quantum dots

CdTe QDs were synthesized as described by Zou et al. [42] with some modifications. Briefly, the NaHTe solution was prepared by mixing $NaHB_4$ (1 mmol) and Te powder (0.4 mmol) in 10 mL of N_2 saturated water at 80 ^oC for 30 min under N_2 flow to get a deep red clear solution. Then, 2.0 mmol of $CdCl_2$ and 4.0 mmol of MPA were mixed in a 50 mL of N_2 saturated solution, and the pH of the solution was adjusted to about 10.0 by dropwise addition of 1.0 M NaOH solution with stirring. Under stirring, 2.0 mL of freshly prepared NaHTe solution was added through a syringe into the Cd precursor solution at room temperature (RT). So the molar ratio of Cd:MPA:Te in the reaction solution was 1:2:0.2. Then the reaction mixture was refluxed at 100 ^oC under N_2 protection for 0.5 h.

Coupling c-DNA to CdTe quantum dots (c-DNA@QDs) and Construction of the TiO_2 NTs /aptamer/c-DNA@QD aptasensor

100 μL of 10 μM carboxy-terminated CdTe QDs' suspension was mixed with 400 μL of PBS solution (pH 7.4) containing 4 g L^{-1} EDC and and 2 g L^{-1} NHS for 0.5 h at RT to obtain the activated QDs. Then 20 μL of c-DNA solution (10 nM in 10 mM pH 7.4 PBS) was added to the above solution and left at 4 °C overnight in the dark to allow the coupling of the c-DNA to the QD surface. The resultant c-DNA and CdTe QDs conjugates (c-DNA@QDs) were collected by

centrifugation and washed with 10 mM pH 7.4 PBS for several times. Then they were dispersed in 10 mM pH 7.4 PBS to a final volume of 1 mL and stored at 4 °C for subsequent use.

For Construction of the TiO_2 NTs/aptamer/c-DNA@QD aptasensor, 20μL of thiolated MUC1 aptamer (10μM) was dropped onto the titanium foil with Au/TiO_2 NTs and incubating for 16 h at 4 °C. After modification, the Ti/TiO_2 NTs/aptamer was washed with 10 mM pH 7.4 PBS and incubated in 1.0 mL of 1 mM 6-mercaptohexanol (MCH) solution for 1 h at RT to block the unmodified region of the TiO_2 NTs. Then a 20μL droplet of c-DNA@QDs conjugates solution was covered onto the titanium foil with TiO_2 NTs/aptamer and kept for 2 h at RT to obtain the TiO_2 NTs/aptamer/c-DNA@QD aptasensor (Fig. 1). Finally the prepared aptasensor was washed with 10 mM pH 7.4 PBS for several times and stored at 4 °C for subsequent use.

Electrochemical and photoelectrochemical measurements

All electrochemical and photoelectrochemical measurements were carried out in air-saturated PBS (10 mM, pH 7.4) on a CHI 1240B electrochemical workstation (Shanghai Chenhua Co., Ltd., China) with a conventional three-electrode system, where the titanium foil with TiO_2 NT/aptamer/c-DNA@QD aptasensor was employed as the working electrode, a Pt wire was served as counter electrode, and a saturated calomel electrode (SCE) was used as reference electrode. A 500 W Xe lamp was used as the irradiation source fitted with a 420 nm UV filter (Zolix, China). A mechanical shutter was used to control the light on and off, and the photocurrent was detected with electrochemical workstation at a bias potential. When detecting the content of MUC1, the photocurrent of the TiO_2 NTs/aptamer/c-DNA@QD aptasensor was first detected under the irradiation of visible light which value was I_0. Then, the aptasensor was immersed in the sample solution containing MUC1 with various concentrations (10 mM PBS pH 7.4) and kept at

RT for 0.5 h, followed by a washing with 10 mM pH 7.4 PBS to remove free c-DNA@QDs and nonspecific bound of MUC1 and detection of the photocurrent value, which was *I*. So the concentration of MUC1 could be detected by the photocurrent change value of the aptasensor ($\Delta I=I_0-I$).

Analysis of human serum samples

In the 1.00 mL of the healthy human serum sample (obtained from Xuzhou Central Hospital, P.R. China), a 0.5 mL of of trichloroacetic acid (4 wt% in 10 mM pH 7.4 PBS) was added, stirred, and centrifuged at 4000 rpm for 10 min. The supernatant fluid was diluted to 20 mL with 10 mM pH 7.4 PBS. The concentration of MUC1 in the pretreated serum sample was detected by PEC with the aptasensor. At the same time, a recovery test was carried out in accordance with the same procedure to demonstrate the validity of the proposed aptasensor. The results of applied standard addition method were reported in the supporting information (Table S1).

Results and discussion

Characterization of the prepared TiO_2 NTs and CdTe QDs

For construction of Ti/TiO_2 NTs/aptamer/c-DNA@QD aptasensor, we first prepared TiO_2 NTs by the electrochemical anodization technique. As shown in Fig. 2A, when the anodization potential was 30 V at an anodization time of 4 h, the prepared TiO_2 NTs have an average length of 3.5 μm and the inner diameter of ~90 nm. For improving the electrical conductivity and biocompatibility of TiO_2 NTs,[29] Au nanoparticles (AuNPs) electrodeposited were uniformly dispersed on the inner wall of TiO_2 NTs with an average size of 5 nm (Fig. 2B), which could be used for effectively immobilizing MUC1 aptamers by Au-S band. Meanwhile, CdTe QDs synthesized in the work exhibited a characteristic UV-vis absorption at 553 nm (curve a in the Figure S1A). And,

according to following the expression (Equation 1), [43]

$$D = (9.8127 \times 10^{-7})\lambda^3 - (1.7147 \times 10^{-3})\lambda^2 + 1.0064\lambda - 194.84 \quad (1)$$

where D was the diameter (nm) and λ (nm) was the wavelength maximum corresponding to the absorption peak of the QDs, the particle size of the CdTe QDs was calculated to be ~3.3 nm, which was found in good agreement with the size observed by TEM image (Fig. 2C). In addition, the majority of the CdTe QD particles were between 2.5 nm and 4.0 nm and the median size of the whole population is 3.5 nm, indicating the uniform distribution of CdTe QD particles (Fig. 2D). Furthermore, CdTe QDs had a typical absorption peak at 553 nm in the visible light region, and had a photoluminescence (PL) intensity at the peak of 619 nm under the excitation of 500 nm (Fig. S1A), which indicate the electron transfer from the valence band (VB) to conduction band (CB) of QDs would be easy to occur under the visible light irradiation and generate electron-hole pairs, which made CdTe QDs used as excellent photosensitizer.

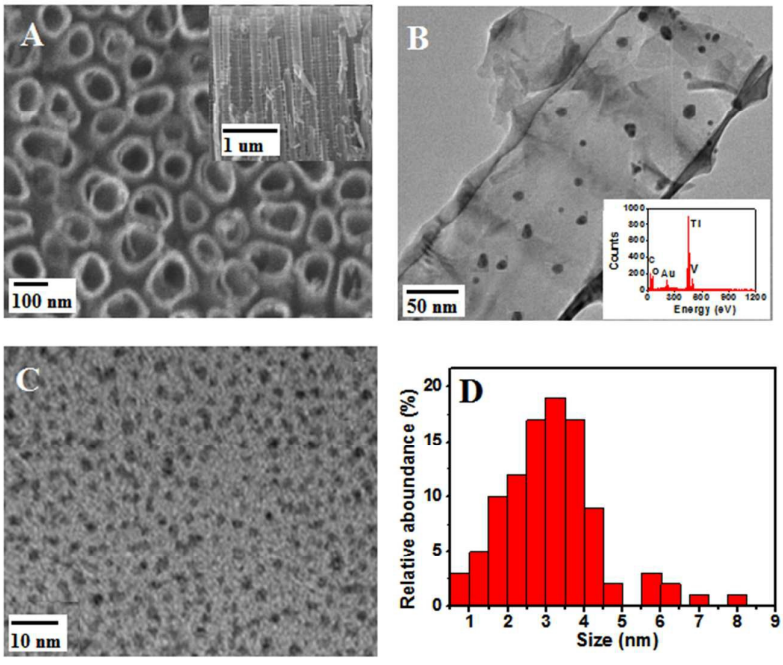

Fig. 2 (A) FESEM top-view image of TiO_2 NTs and corresponding cross section image (Inset); (B)

TEM image of AuNPs-coated TiO_2 NTs and corresponding energy dispersive spectrogram (Inset); (C) TEM image of CdTe QDs; (D) size distribution histograms for CdTe QDs.

Photoelectrochemical property of TiO_2 NTs and TiO_2 NT/aptamer/c-DNA@QD aptasensor

Fig. 3 showed the photocurrent action spectra of TiO_2 NTs and TiO_2 NT/aptamer/c-DNA@QD recorded under intermittent irradiation at the applied potential of 0.1 V. For TiO_2 NTs (Fig. 3A), a typical behavior was observed with the anodic photocurrent disappearing at wavelengths above 380 nm, as established in the literature. [32-34] However, after CdTe QDs immobilized on the TiO_2 NTs by the hybridization of MUC1 aptamer and c-DNA, QD/TiO_2 NTs exhibited a stronger photocurrent response and the photocurrent response was extended to visible light down to ~550 nm (Fig. 3B). This typical difference could be explained by their energy levels. The CB and VB of TiO_2 NTs were located at -4.21 and -7.41 eV, respectively. And the band gap of TiO_2 NTs was ~3.2 eV, which could only utilize the UV part of solar radiation, [34] limiting the extensive application, such as in biosensing. In addition, the band gap of CdTe QDs was calculated as 2.24 eV according to the UV-vis absorption spectrum (Fig. S1A). Coupled with the information that the electrochemical reduction peak of CdTe QDs on the ITO electrode was observed at -0.82 V (vs. SCE, Fig. S1B), the CB and VB positions of CdTe QDs could be quantified as -3.92 eV and -6.18 eV, respectively. Under the light irradiation, CdTe QDs excited electrons from the CB to the VB and generate holes at the VB. The CB of TiO_2 NTs was more positive than that of CdTe QDs, [44] resulting in a local electric field. As a result, the excited electrons could quickly transfer from QDs to TiO_2 conduction band. Furthermore, the tubular structure of TiO_2 was helpful for separating and transferring photoinduced electrons to the titanium substrate foil, [45] which contributed to the increasing photocurrent (Fig. 4).

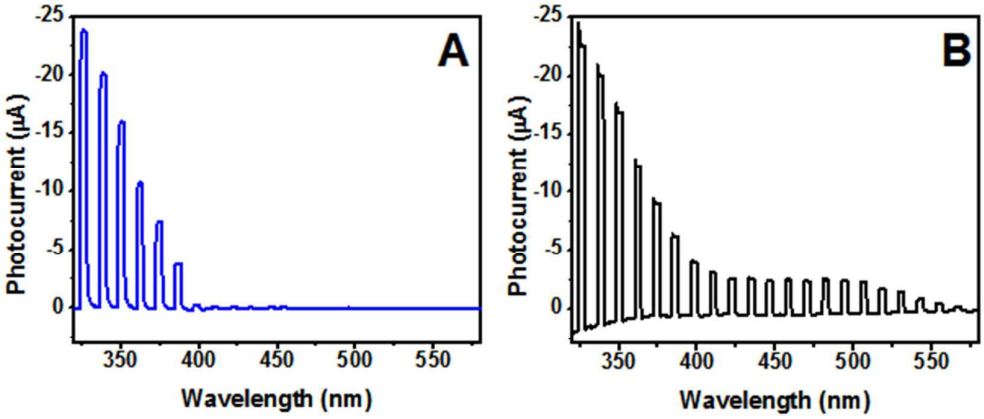

Fig. 3 Photocurrent measured under intermittent irradiation as a function of irradiation wavelength (without correction for the change of light intensity). (A) TiO_2 NTs; (B) TiO_2 NT/aptamer/c-DNA@QD aptasensor. Applied potential, 0.1 V; TiO_2 NTs prepared at anodization potential of 30 V and anodization time of 4 h.

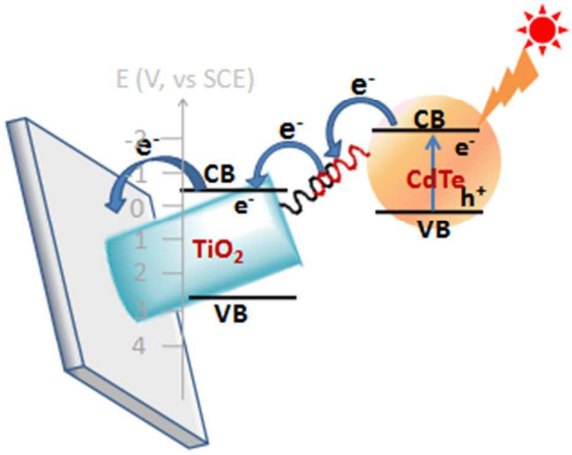

Fig. 4 Scheme diagram of the electron transfer steps of the TiO_2 NT/aptamer/c-DNA@QD on titanium substrate foil upon visible light irradiation.

Effect of the TiO_2 NTs morphology on the photocurrent response of TiO_2 NT/aptamer/c-DNA@QD

According to our previous report, [29] in the work, the TiO_2 NTs were prepared when the anodization potential was fixed at 30 V, and the anodization time was 1.0, 2.0, 3.0, 4.0 and 8.0 h,

which were referred to TNT-1, TNT-2, TNT-3, TNT-4, and TNT-8 respectively. To investigate the effects of TiO_2 NTs morphology on the photocurrent response of the aptasenor, a conventional electrochemical system was employed to measure the photocurrent change by linear sweep voltammetry (LSV) at a selected potential window of -1.0-1.0 V. As shown in Fig. 5, when CdTe QDs were immobilized on the titanium foil substrate directly, under the irradiation of visible light, the generated photocurrent was very little at the applied potential of -1.0-1.0 V (Fig. 5A). However, there had obvious photocurrents generated for TiO_2 NT/aptamer/c-DNA@QD when the applied potential more positive than 0.0 V, which indicated the Ti/TiO_2 NT/aptamer/c-DNA@QD electrode was a typical photoanode. With the increase of tube length of TiO_2 NTs (From TNT-1 to TNT-8), the photocurrent increased in the applied potential range of 0-1.0 V (Fig. 5 B-F). It was because that, the prepared TiO_2 NTs were well-aligned vertically on the titanium foil substrate, which not only provided accessible accesses for immobilizing high amount of QDs, but promoted the directional charge transport due to the one-dimensional features of the tubes, [45, 46] leading to the increase of photocurrent. When the TNT-4 TiO_2 NTs were used for construction of the aptasensor, the generated photocurrent was relatively stable at the applied potential range of 0.5 to 1.0 V (Fig. 5E), which was important for the construction of a photoelectrochemical aptasensor. However, for the TiO_2 NTs with longer tube length, the photocurrent was relatively high but not stable instead, such as for TNT-8 TiO_2 NTs (Fig. 5F). Therefore, the TNT-4 TiO_2 nanotube arrays and the applied potential of 0.6 V were used in the subsequent experiments.

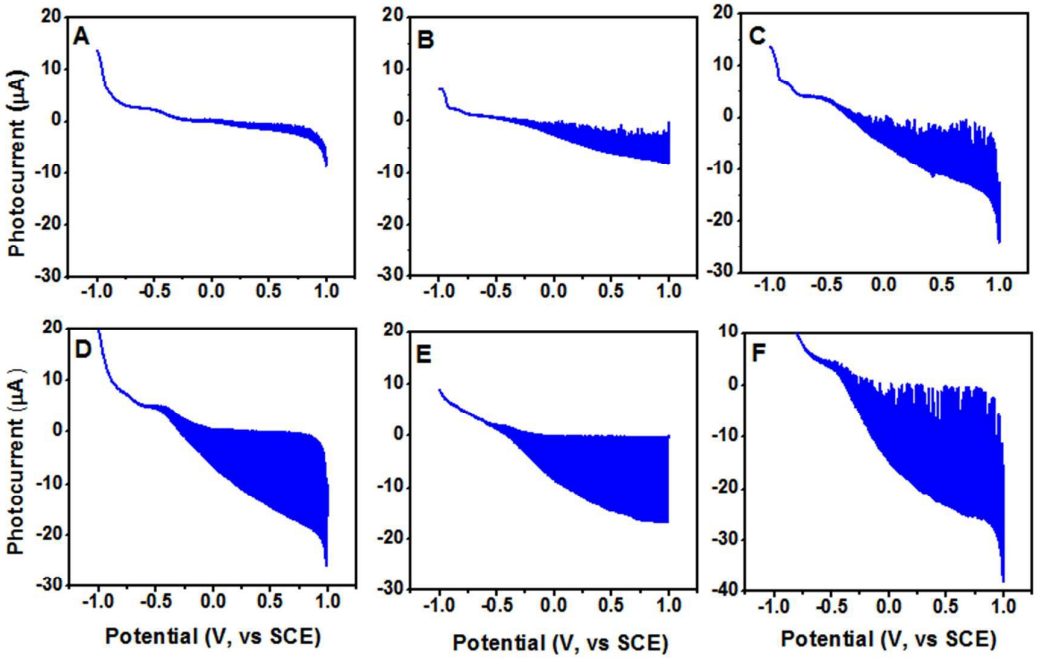

Fig. 5 Photocurrent responses of Ti/aptamer/c-DNA@QD (A) and TiO_2 NT/aptamer/c-DNA@QD aptasensor (B-F) at different bias potential under the irradiation of visible light. Potential was scanned from -1.0 to 1.0 V with 0.1 V s^{-1} of scan rate. The TiO_2 NTs were referred to TNT-1 (B), TNT-2 (C), TNT-3 (D), TNT-4 (E) and TNT-8 (F), which was prepared at the anodization potential of 30 V, and the anodization time was 1.0, 2.0, 3.0, 4.0 and 8.0 h, respectively.

Effect of different chain lengths of c-DNA on the photocurrent response of TiO_2 NT/aptamer/c-DNA@QD aptasensor

It was known that DNA could transport electrical current as efficiently as a good semiconductor, which would be useful in the design of future electronic devices based on DNA molecules, [47] and there had many factors that affect the conductivity, including ambient surroundings, and the distance between the donor and acceptor sites. [48, 49] In this work, the distance from electron donor QDs to acceptor TiO_2 NTs could be adjusted by c-DNA chain length. To study the effect of the distance between the donor and acceptor on photocurrent response of TiO_2 NT/aptamer/c-DNA@QD aptasensor, c-DNA chains with different lengths were designed to

hybridize MUC1 aptamer for construction of the aptasensor, which were denoted as T1, T2, T3, T4, T5 and T6 containing the c-DNA with chain length of 27-mer, 42-mer, 72-mer, 102-mer, 132-mer and 312-mer, respectively). As shown in Fig. 6A, with the increase of c-DNA chain length from 27-mer to 72-mer, the photocurrent basically did not change. However, further increasing of the chain length of DNA hybridization more than 102-mer, the photocurrent decreased significantly, and was very little when the chain length of DNA hybridization was at 312-mer. Therefore, we speculated that the chain length of c-DNA has great influence on the electron transport property of DNA. When the chain length was relatively short, such as 27-mer, 42-mer and 72-mer, DNA had very strong electron transfer ability, which could transport the photoinduced electron from the CB of CdTe QDs to the TiO_2 NTs. However, if the chain length of DNA was too long, such as 312-mer, it would block the electron transfer. Furthermore, according to the distance of about 10 bases of DNA 3.4 nm, [50] the electron transfer performance of DNA would significantly weaken when the chain length of DNA hybridization was more than 38 nm. In addition, to study the sensitivity of TiO_2 NT/aptamer/c-DNA@QD aptasensor, the photocurrent responses of the aptasensor with c-DNA of two different chain lengths were compared after adding the same amount of MUC1 target. The results showed that (Fig. 6B), when the chain length of DNA was relatively short, such as 27-mer, the photocurrent reduced slowly due to the steric hindrance of c-DNA@QDs on the combination of MUC1 and its aptamer (curve a of Fig. 6B). The photocurrent signal was decreased by 7.2% in 20 min after adding 50 nM of MUC1. However, the photocurrent signal was decreased by 23.5% in 20 min when the chain length of DNA was 72-mer. Therefore, in the subsequent experiments, the c-DNA with the chain length of 72-mer was used for construction of TiO_2 NT/aptamer/c-DNA@QD aptasensor to determine the MUC1 target.

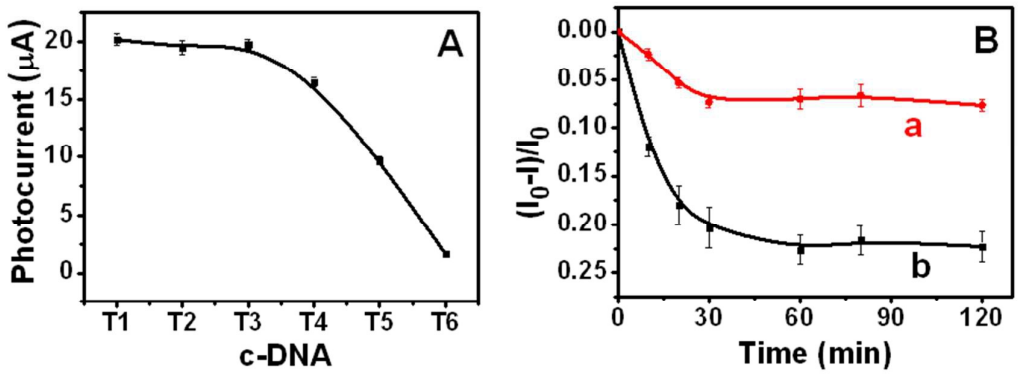

Fig. 6 (A) Effects of different distances of TiO_2 NTs and CdTe QDs on the photocurrent response of TiO_2 NT/aptamer/c-DNA@QD aptasensor, T1, T2, T3, T4, T5 and T6 represented the aptasensor which contained the c-DNA with chain length of 27-mer, 42-mer, 72-mer, 102-mer, 132-mer and 312-mer, respectively. (B) Photocurrent response change of TiO_2 NT /aptamer/c-DNA@QD aptasensor with 27-mer (a) or 72-mer (b) c-DNA chain after incubation with 50 nM of MUC1.

Effect of pH value on the TiO_2 NT/aptamer/c-DNA@QD aptasensor

The pH value of PBS solution had a great effect on the photoelectrochemical behavior of aptasensor. As shown in Fig. S2, the influence of pH value on the photocurrent response change ($\Delta I=I_0-I$) of the aptasensor was investigated in the pH range from 5.0 to 9.0 when the aptasensor was immersed in the 10 mM PBS solution containing 100 nM MUC1. It was found that the ΔI increased with the increment of pH value from 5.0 to 7.4 and decreased thereafter. Therefore, the optimal photocurrent response change ΔI was achieved at pH 7.4. The reason might be that, the higher or lower pH environments may damage the stability and activity of the immobilized biomolecules, and then influence the life time of the aptasensor. [51] Therefore, the pH value of 7.4 was chosen in the subsequent experiments.

Analytical performance of the TiO_2 NT/aptamer/c-DNA@QD aptasensor for MUC1

biosensing

In the work, when different concentration of the target MUC1 was introduced in the electrolyte solution, the MUC1 aptamer on the TiO_2 NTs preferred to form the aptamer-MUC1 complex, which resulted in the dehybridization of aptamer/c-DNA and the c-DNA@QD released into the solution, so leading to the reduce of photocurrent of TiO_2 NT/aptamer/c-DNA@QD system. As shown in Fig. 7A, the decrease in photocurrent was dependent on the MUC1 concentration. The relative change of photocurrent intensity (ΔI) was linear proportional to the concentration of MUC1 in the ranges of 2 nM to 0.2 μM as shown in Fig. 7B, which would be capable to accommodate the monitoring of MUC1 in biological samples of healthy and cancer-affected patients because the cut-off concentration of MUC1 for a normal healthy human is generally accepted to be approximately 5 μM. [9] And a limit of detection (LOD) of such aptasensor based on a signal-to-noise ratio of 3 was 0.52 nM, which was much lower compared to many other reports. For example, He et al. [5] developed a fluorescent aptasensor for MUC1 detection by using a dye-labeled aptamer and graphene oxide (GO) with a LOD of 28 nM. Hu et al. [12] developed a multiple signal amplification strategy for detection of MUC1 based on HO-functionalized AuNPs amplification coupled with enzyme-linkage reactions with a LOD of 2.2 nM. Ma et al. [15] reported an aptamer-based electrochemical biosensor for the quantitative determination of mucin 1 (MUC1) with a LOD of 50 nM, which based on the analyte-binding induced, global-scale conformational change of electrode-bound anti-MUC1 DNA aptamers. Liu et al. [52] developed an electrochemical impedimetric aptasensor based on gold nanoparticles (AuNPs) signal amplification for the ultrasensitive detection of tumor markers, which LOD was 0.1 nM. And Florea et al. [53] developed two electrochemical approaches for Mucin1 (MUC1) tumor marker, which LOD was 0.19 nM

with anti-MUC1 antibody based biosensor and 0.07 nM with anti-MUC1 aptamer based biosensor, respectively. In addition, the developed sensitive aptasensor for the MUC1 based on PEC method has plenty of advantages such as low background, low potential different from electrochemical method, which lead to a good analytical performance and high selectivity, and could offer a promising feature for the analytical application for wider tumor markers biosensing in complex biological samples.

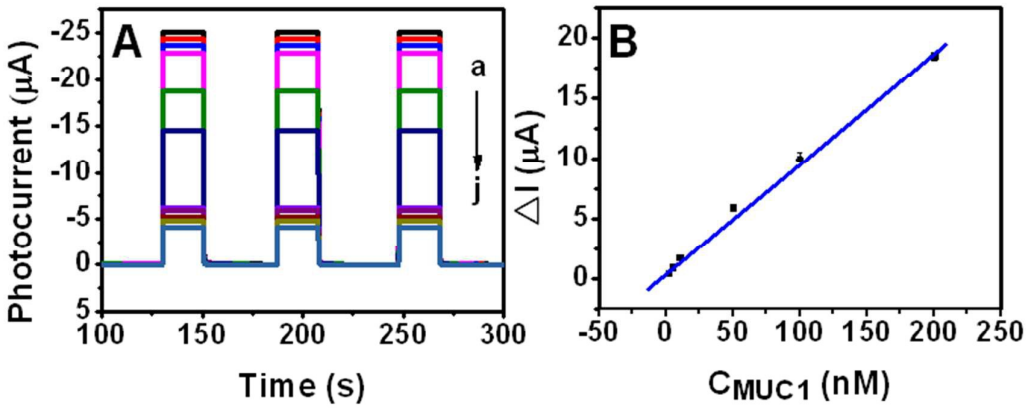

Fig. 7 (A) Photocurrent responses of TiO_2 NT/aptamer/c-DNA@QD aptasensor under the irradiation of visible light in 10 mM pH 7.4 PBS solution containing 0 (a), 0.002 (b), 0.005 (c), 0.01 (d), 0.05 (e), 0.1 (f), 0.2 (g), 0.3 (h), 0.5 (i), 1.0 (j) and 2.0 μM (k) of MUC1, respectively. (B) Calibration curve of photocurrent response change of the aptasensor (ΔI) versus MUC1 concentration (C_{MUC1}) in the ranges of 2 nM to 200 nM. Applied potential, 0.6 V.

Specificity, reproducibility and stability of the aptasensor

In order to evaluate the specificity of TiO_2 NT/aptamer/c-DNA@QD aptasensor for MUC1, carcinoembryonic antigen (CEA), myoglobin (MYO), tumor necrosis factor-α (TNF-α), or albumin, one of major proteins in human serum, was selected to replace MUC1. As shown in Fig. S3, incubation of the TiO_2 NT/aptamer/c-DNA@QD electrode with 1 μM of CEA, MYO, TNF-α or 1 mM of albumin did not produce significant changes of photocurrent response as compared to

the case of MUC1 (10 nM). In addition, to examine the effect of possible interferences from real serum samples on the detection of MUC1, calibration curves of MUC1 were constructed when the aptasensor was in the serum solution or PBS solution containing different concentration of MUC1, and the results showed that (Fig. S4), the determination of MUC1 was almost same in the serum solution or PBS solution. All of these results strongly demonstrated that that the developed aptasensor has a sufficient specificity to the target molecule, MUC1.

Furthermore, the reproducibility of the aptasensor for MUC1 biosensing was studied. For the same aptasensor, the relative standard deviation (RSD) of the photocurrent response to 10 nM of MUC1 was evaluated to be 3.7% for 11 successive measurements. And for different aptasensors the sensor-to-sensor reproducibility was also examined between six aptasensors and the RSD was calculated to be 7.2%, which indicated good reproducibility of the aptasensor.

Moreover, the photocurrent response of the TiO_2 NT/aptamer/c-DNA@QD aptasensor did not change significantly within 5 h at regular intervals of 30 min when it was incorporated in the 10 mM pH 7.4 PBS. In addition, the detection stability of the aptasensor to actual target MUC1 was identified. In details, the photocurrent response of the constructed aptasensor to 10 nM of MUC1 was detected at regular intervals of every other day after 10 days' storage in 10 mM pH 7.4 PBS at 4 ^{o}C. In the process, the used aptasensor was regenerated by 5.0 M urea for subsequent use. The results showed that, the aptasensor could retain ~89% of its initial activity after 10 days' usage and storage, which might be attributed to the fact that the aptasensor provided a biocompatible microenvironment for aptamer molecules to stabilize their bio-identification activity, and indicated the aptasensor had a good operational stability and continuous usage for days.

Analysis of human serum sample and regeneration of the aptasensor

In order to reduce the matrix effect, the serum samples were processed and diluted with 20 times by 10 mM pH 7.4 PBS according to the experimental procedure. The results showed that (Table S1), the concentration of MUC1 in healthy human serum was very low that was less than the LOD of the developed aptasensor. To evaluate the accuracy of the aptasensor, we carried out standard addition method. As seen in Table S1, when the added concentration of MUC1 was 10, 50, 100 nM into the above human serum, which were lower than the cut-off concentration of MUC1, the relative standard deviation values of the analytical results were less than 4.3%, and the recoveries for the spiked samples ranged from 98.5% to 105.2%, which implied the aptasensor had a good accuracy, was fully applicable to detection of clinical serum samples including pathologic or non-pathologic, and indicated a promising feature for the analytical application in complex biological samples.

Furthermore, the proposed aptasensor could be regenerated for repeated use. In details, after each determination, the aptasensors were immersed into 5.0 M urea for 10 min at room temperature to disassociate the aptamer-MUC1 complex and then washed with 10 mM pH 7.4 PBS. The aptasensor was regenerated and could maintain ~83% activity upon repetition of these regeneration steps for 10 cycles, showing an acceptable reusability (Fig. S5).

Conclusions

In the present work, selecting titanium foil as substrate, we constructed a sensitive TiO_2 NT/aptamer/c-DNA@QD aptasensor for MUC1. In which, the photosensitizer CdTe QDs were immobilized on the TiO_2 NTs by the hybridization of c-DNA and aptamer. Due to the the excellent photosensitivity of CdTe QDs and electrical conductivity of DNA chain, the proposed aptasensor had good phocurrent response under the irradiation of visible light. In addition, the photocurrent

response could be effectively regulated by changing the tube length of TiO_2 NTs and the chain length of DNA linking QDs and TiO_2 NTs. Furthermore, the concentration of MUC1 could be determined by the aptasensor with a photoelectrochemical approach, which exhibited the wider linear range, satisfying detection limit, good reproducibility and stability. Therefore, the developed aptasensor could offer a promising feature for the analytical application in complex biological samples, and the proposed method could also provide promising platforms for other biosensing and bioelectronics applications.

Acknowledgements

The authors gratefully acknowledge the financial support provided by the project funded by the Priority Academic Program Development of Jiangsu Higher Education Institutions, Brand Major of Universities in Jiangsu Province, the National Natural Science Foundations of China (21205052), the Science and Technology Project of Xuzhou City (XF11C050), the Natural Science Foundation of Jiangsu Normal University (15XLR007), and the Natural Science Foundation of Jiangsu Education Committee (11KJB150018).

Reference

1 M. A. Hollingsworth and B. J. Swanson, *Nat. Rev. Cancer*, 2004, **4**, 45-60.

2 M. Andrianifahanana, N. Moniaux and S. K. Batra, *BBA-Rev. Cancer*, 2006, **1765**, 189-222.

3 S. Senapati, S. Das and S. K. Batra, *Trends Biochem. Sci.*, 2010, **35**, 236-245.

4 S. Muller, K. Alving, J. Peter-Katalinic, N. Zachara, A. A. Gooley and F. G. Hanisch, *J. Biol. Chem.*, 1999, **274**, 18165-18172.

5 Y. He, Y. Lin, H. W. Tang and D. W. Pang, *Nanoscale*, 2012, **4**, 2054-2059.

6 C. S. M. Ferreira, K. Papamichael, G. Guilbault, T. Schwarzacher, J. Gariepy and S. Missailidis,

Anal. Bioanal. Chem., 2008, **390**, 1039-1350.

7 J. V. Van den Bossche, W. T. Al-Jamal, B. W. Tian, A. Nunes, C. Fabbro, A. Bianco, M. Prato and K. Kostarelos, *Chem. Commun.*, 2010, **46**, 7379-7381.

8 M. Begum, S. Karim, A. Malik, R. Khurshid, M. Asif, A. Salim, S. A. Nagra, A. Zaheer, Z. Iqbal, A. M. Abuzenadah, M. H. Alqahtani and M. Rasool, *Asian Pac. J. Cancer P.*, 2012, **13**, 5257-5261.

9 A. K. H. Cheng, H. P. Su, Y. A. Wang and H. Z. Yu, *Anal. Chem.*, 2009, **81**, 6130-6139.

10 E. Gheybi, J. Amani, A. H. Salmanian, F. Mashayekhi and S. Khodi, *Tumor Biol.*, 2014, **35**, 11489-11497.

11 W. Wei, D. F. Li, X. H. Pan and S. Q. Liu, *Analyst*, 2012, **137**, 2101-2106.

12 P. Wu, Y. Gao, H. Zhang and C. X. Cai, *Anal. Chem.*, 2012, **84**, 7692-7699.

13 L. H. Tan, K. G. Neoh, E. T. Kang, W. S. Choe and X. D. Su, *Anal. Biochem.*, 2012, **421**, 725-731.

14 R. Hu, W. Wen, Q. L. Wang, H. Y. Xiong, X. H. Zhang, H. S. Gu and S. F. Wang, *Biosens. Bioelectron.*, 2014, **53**, 384-389.

15 F. Ma, C. Ho, A. K. H. Cheng and H. Z. Yu, *Electrochim. Acta*, 2013, **110**, 139-145.

16 A. D. Ellington and J. W. Szostak, *Nature*, 1990, **346**, 818-822.

17 C. Tuerk and L. Gold, *Science*, 1990, **249**, 505-510.

18 C. Y. Deng, J. H. Chen, L. H. Nie, Z. Nie and S. Z. Yao, *Anal. Chem.*, 2009, **81**, 9972-9978.

19 S. F. Liu, Y. Wang, C. X. Zhang, Y. Lin and F. Li, *Chem. Commun.*, 2013, **49**, 2335-2337

20 Y. Liang, B. Kong, A.W. Zhu, Z. Wang and Y. Tian, *Chem. Commun.*, 2012, **48**, 245-247.

21 D. Chen, H. Zhang, X. Li and J. H. Li, *Anal. Chem.*, 2010, **82**, 2253-2261.

22 W. W. Zhao, Z. Y. Ma, P. P. Yu, X. Y. Dong, J. J. Xu, H. Y. Chen, *Anal. Chem.*, 2012, **84**, 917-923

23 Q. M. Shen, X. M. Zhao, S. W. Zhou, W. H. Hou and J. J. Zhu, *J. Phys. Chem. C*, 2011, **115**, 17958-17964.

24 J. Tanne, D. Schafer, W. Khalid, W. J. Parak and F. Lisdat, *Anal. Chem.*, 2011, **83**, 7778-7785.

25 X. R. Zhang, Y. Q. Zhao, S. G. Li and S. S. Zhang, *Chem. Commun.*, 2010, **46**, 9173-9175.

26 W. Tremel, *Angew. Chem. Int. Ed.*, 1999, **38**, 2175-2179.

27 R. Wang, C. Ruan, D. Kanayeva, K. Lassiter and Y. Li, *Nano Lett.*, 2008, **8**, 2625-2631.

28 D. Chen, G. Wang and J. H. Li, *J. Phys. Chem. C*, 2007, **111**, 2351-2367.

29 J. S. Lu, H. N. Li, D. M. Cui, Y. J. Zhang and S. Q. Liu, *Anal. Chem.*, 2014, **86**, 8003-8009.

30 S. Q. Liu and A. C. Chen, *Langmuir*, 2005, **21**, 8409-8413.

31 A. K. M. Kafi, G. Wu and A. Chen, *Biosens. Bioelectron.*, 2008, **24**, 566-571.

32 Y. Tian and T. Tatsuma, *J. Am. Chem. Soc.*, 2005, **127**, 7632-7637.

33 T. Tachikawa, N. Wang, S. Yamashita, S. C. Cui and T. Majima, *Angew. Chem., Int. Ed.*, 2010, **49**, 8593-8597.

34 T. Tachikawa, S. Yamashita and T. Majima, *J. Am. Chem. Soc.*, 2011, **133**, 7197-7204.

35 Q. Y. Wang, X. C. Yang, X. L. Wang, M. Huang and J. W. Hou, *Electrochim Acta*, 2012, **62**, 158-162.

36 U. Kang and H. Park, *Appl Catal B- Environ.*, 2013, **140-141**, 233-240.

37 W. Zhao, Y. L. Sun and F. N. Castellano, *J. Am. Chem. Soc.*, 2008, **130**, 12566-12567.

38 H. Y. Wang, G. M. Wang, Y. C. Ling, M. Lepert, C. C. Wang, J. Z. Zhang and Y. Li, *Nanoscale*, 2012, **4**, 1463-1466.

39 X. Yan, X. Cui, B. S. Li and L. S. Li, *Nano Lett.*, 2010, **10**, 1869 -1873.

40 V. Gupta, N. Chaudhary, R. Srivastava, G. D. Sharma, R. Bhardwaj and S. Chand, *J. Am. Chem. Soc.*, 2011, **133**, 9960- 9963.

41 J. A. Seabold, K. Shankar, R. H. T. Wilke, M. Paulose, O. K. Varghese, C. A. Grimes and K. S. Choi, *Chem. Mater.*, 2008, **20**, 5266-5273.

42 L. Zou, Z. Y. Gu, N. Zhang, Y. L. Zhang, Z. Fang, W. H. Zhu and X. H. Zhong, *J. Mater. Chem.*, 2008, **18**, 2807-2815.

43 W. W. Yu, L. H. Qu, W. Z. Guo and X. G. Peng, *Chem. Mater.*, 2003, **15**, 2854-2860.

44 Y. J. Li, M. J. Ma and J. J. Zhu, *Anal. Chem.*, 2012, **84**, 10492-10499

45 H. Zhang, X. Quan, S. Chen, H. T. Yu and N. Ma, *Chem. Mater.*, 2009, **21**, 3090-3095.

46 Q. Kang, L. X. X. Yang, Y. F. Chen, S. L. Luo, L. F. Wen, Q. Y. Cai and S. Z. Yao, *Anal. Chem.*, 2010, **82**, 9749-9754.

47 K. Keren, R. S. Berman, E. Buchstab, U. Sivan and E. Braun, *Science*, 2003, **302**, 1380-1382

48 H. W. Fink and C. Schonenberger, *Nature*, 1999, **398**, 407-410.

49 Y. T. Long, E. Abu-Irhayem and H. B. Kraatz, *Chem. Eur. J.*, 2005, **11**, 5186-5194.

50 X. Y. Sun, B. Liu, Y. F. Sun and Y. M. Yu, *Biosens. Bioelectron.*, 2014, **61**, 466-470.

51 Y. Y. Cai, H. Li, Y. Y. Li, Y. F. Zhao, H. M. Ma, B. C. Zhu, C. X. Xu, Q. Wei, D. Wu and B. Du, *Biosen. Bioelectron.*, 2012, **36**, 6-11.

52 X. Liu, Y. Qin, C. Y. Deng, J. Xiang and Y. J. Li, *Talanta*, 2015, **132**, 150-154.

53 A. Florea, A. Ravalli, C. Cristea, R. Sandulescu and G. Marrazza, *Electroanalysis*, 2015, **27**, 1594-1601.